Understanding the reshaping of fluorinated polyester vitrimers by kinetic and DFT studies of the transesterification reaction

Sébastien Lemouzy, Florian Cuminet, Dimitri Berne, Sylvain Caillol, Vincent Ladmiral, Rinaldo Poli, Eric Leclerc

Understanding the reshaping of fluorinated polyester vitrimers by kinetic and DFT studies of the transesterification reaction

Sébastien Lemouzy,[a] Florian Cuminet,[a] Dimitri Berne,[a] Sylvain Caillol,[a] Vincent Ladmiral,[a] Rinaldo Poli*[b,c] and Eric Leclerc*[a]

[a] Dr. S. Lemouzy, Mr. F. Cuminet, Mr. D. Berne, Dr. S. Caillol, Dr. V. Ladmiral, Dr. E. Leclerc
ICGM, Univ Montpellier, CNRS, ENSCM
34293 Montpellier, France
E-mail: eric.leclerc@enscm.fr

[b] Prof. R. Poli
CNRS, LCC (Laboratoire de Chimie de Coordination), UPS, INPT, Université de Toulouse
205 route de Narbonne
F-31077 Toulouse, Cedex 4, France

[c] Prof. R. Poli
Institut Universitaire de France
1, rue Descartes
75231 Paris, France

E-mail: Rinaldo.poli@lcc-toulouse.fr

Supporting information for this article is given via a link at the end of the document.

Abstract: Vitrimers are a third class of polymers gathering the mechanical properties and solvent resistance of 3D thermosets and the reprocessability of thermoplastics. This unique behaviour is due to the triggering of certain covalent exchange reactions that allow the network to rearrange upon application of a stimulus. The constitutive feature of vitrimers is the adoption of a glass-like viscosity during the rearrangement of the network, often due to an associative mechanism for the exchange reaction. Transesterification networks are one of the most studied type of vitrimers that usually require the incorporation of a catalyst, implying the associated drawbacks. Our group recently reported catalyst-free transesterification vitrimers in which the ester functions are particularly reactive thanks to the presence of fluorine atoms in α- or β-position. In the present contribution, we present parallel DFT calculations and an experimental kinetic study on model molecules in order to quantitatively assess the effect of neighbouring fluorinated groups on the transesterification reaction rate.

Introduction

For almost two decades, the frontier between the two traditional categories of polymers, namely thermoplastics and thermosets, has been blurred by the development of vitrimers, a particular class of covalent adaptable networks (CANs).[1] This new breed of organic materials indeed gathers the mechanical and chemical resistance of permanent 3D networks and, to some extent, the reprocessability and recyclability of linear polymers.[2] The peculiar properties of CANs rely on the following simple strategy: the 3D network is composed of covalent links that can be exchanged with other functions or similar links elsewhere in the network upon application of a stimulus (heat or light).[3] A fast and efficient reversible reaction and the availability of the two reactive functions in the network are therefore required to allow the dynamic behaviour of the material at high temperature and its reprocessability.[4]

Organic chemistry is rich of reversible reactions that can be applicable to such a purpose but the Diels-Alder reaction is certainly the most emblematic and was implemented in a CAN as early as 1990.[5] However, the reversibility of the Diels-Alder reaction is based on a dissociative mechanism in which the initial diene and dienophile have to be regenerated before reacting with another partner in the network. Such a mechanism results in a decrease of network connectivity associated to a drop of viscosity when the retro-Diels-Alder process is thermally activated. In contrast, the use of the transesterification reaction in polyester materials gave rise to reshapable polymers with a glass-like linear dependence of the viscosity versus temperature, named "vitrimer" by Leibler *et al.*[6] This peculiar behaviour is linked to the associative nature of the transesterification reaction, which requires the addition of a free alcohol to the ester carbonyl function prior to the release of the initial alkoxy group.[7] Since this seminal work, a considerable variety of reversible reactions was implemented but, despite outstanding properties, the resulting vitrimer materials have not yet led to notable industrial and commercial applications.[8] Long reprocessing times, high temperatures and, in most cases, high catalyst loadings are often required, limiting the applicability of such materials through ageing or catalyst leaching.[7, 9] The development of catalyst-free vitrimers was initiated by work based on vinylogous urethanes, which allowed fast exchange reactions and short reprocessing times in the absence of any additive.[10] This pioneering work was followed by many examples of fast exchange reactions applied to vitrimers,[11] highlighting the strong influence of the molecular reactivity on the material properties.[12] However, the use of a specific, particularly fast, reaction is not the sole strategy to provide additive-free materials: a standard reaction can be accelerated by the use of a catalyst covalently embedded in the network, or more generally by neighboring group participation (NGP) or electronic effects introduced by specific substituents, the latter being sometimes improperly termed “internal

catalysis"[13] The different NGP-activated reactions implemented in additive-free adaptable networks have recently been summarized in a perspective article by our group.[14]

Due to their wide applicability and ease of preparation, polyester networks remain interesting targets and constitute an ideal platform to explore the possibilities of designing additive-free vitrimers.[6, 15] Indeed, most of the polyester vitrimers reported so far, including those described in Leibler's seminal work, require high catalyst loadings. Using internal catalysis or NGP to inherently promote this reaction and trigger a thermally stimulated dynamic exchange is a real challenge.[12] We envisioned that placing a fluorocarbon group in the ester α- or β-position should result in a strong increase of the electrophilicity of the carbonyl group, thanks to the electron-withdrawing effect of the fluorine atoms.[16] Fluorinated carbonyl derivatives are well known to be very reactive electrophiles and, as such, the transesterification reaction may be strongly promoted without the need of additives, or may occur at lower temperatures, relative to that of non-fluorinated analogues. However, to the best of our knowledge, no detailed kinetic study dealing with the transesterification of fluorinated esters is available. The limited interest of this reaction from a synthetic chemist's point of view is probably responsible for this shortcoming.

Our group has recently reported polyester vitrimers featuring two fluorine atoms in α-position the ester functions, which indeed can be reshaped under mild conditions without catalyst and thus confirmed the above-mentioned F-effect hypothesis.[17] Additional work has also revealed that the reshaping of transesterification vitrimers can be accelerated by the introduction of an α-CF_3 group (fluorine atoms in β-position), which was supported by DFT calculations on a model transesterification reaction.[18] Following those initial investigations, we have conducted more extensive DFT calculations in order to quantitatively assess the effect of neighbouring fluorinated groups on the transesterification reaction rate. In addition, we have conducted experimental kinetic studies on model molecules to verify and validate the DFT predictions. We wish to report herein the details of this joint theoretical and experimental study.

Results and Discussion

DFT calculations

Following the recently reported acceleration for the reshaping process in transesterification vitrimers upon introduction of F atoms at the ester α [17] and β[18] positions, it was of interest to use the computational approach to understand the origin of this effect and to predict how to possibly further improve the transesterification rate.

Transesterification can in principle follow two different pathways, a direct one (single transition state) and a two-step pathway with formation of a tetrahedral intermediate (paths *a* and *b* in Scheme 1). Both have been investigated in previous computational contributions.[19] In each pathway, the carbonyl group may be activated by interaction of the O atom with a Brønsted or Lewis acid catalyst and possible additional assistance may be provided by proton relay molecules through H-bond chains. One recent contribution has specifically addressed a model system of the metal-catalyzed transesterification in vitrimers.[19e] A comparative investigation of the direct and two-step pathways, with extensive analysis of the H-bond chain assistance, has been presented for a mechanistically related reaction (the carbonate ester amination),[20] yielding activation barriers that are highly dependent on the number of proton relay molecules in the chain. Since the present investigation only aims at examining the relative effect of the F substitution, which presumably is mostly expressed at the electronic level, we have opted to limit the investigation to the two step-pathway. For simplicity, we have examined simple model molecules and a degenerate exchange (identical incoming and outgoing alcohol). Therefore, only one transition state is of interest, because the alcohol elimination (second step) is the microscopic reverse of the alcohol addition (first step). A comparison of the activation barriers for the model degenerative exchange of the propionate esters $CX_3CH_2COOCH_3$ (X = H, F) with methanol has already been reported.[18] In the present contribution, we have expanded this investigation to systems having a variable number of F atoms at the ester α and β positions, R_FCOOCH_3 ($R_F = CH_{3-n}F_nCH_{2-m}F_m$; *n* = 0-3, *m* = 0-2), as well as on the alcohol ($CH_{3-n}F_nOH$, n = 0-3).

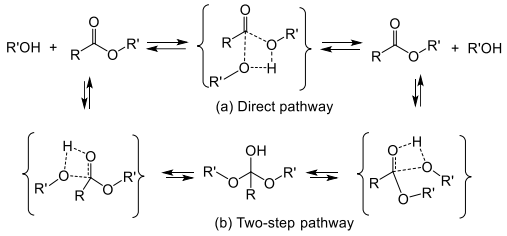

Scheme 1. Possible transesterification pathways (degenerative exchange).

The calculations were carried out with the BP86 functional with corrections for dispersion forces and other effects (see the computational details). The vitrimer synthesis and reshaping occurs in the absence of solvent, but a solvation correction was nevertheless carried out using an arbitrary permittivity value (ε) of 10. The permittivities of methyl and ethyl acetate are 6.7 and 6.0,[21] while those of the corresponding F-substituted esters do not appear to have been measured, but several trifluoromethyl derivatives have values around 10 (trifluorotoluene, 9.1; cyclo-hexyltrifluoromethane: 11).[22] In addition, a slight ε increase may be related to the presence of free alcohol. All values reported below are standard Gibbs energies (25 °C, 1 M concentration).

Preliminary investigations on acetate esters.

Initial calculations were carried out on the degenerative transesterification of differently F-substituted methyl acetates ($CH_{3-n}F_nCOOCH_3$, *n* = 0-3), with only the reacting alcohol molecule in the calculations. The alcohol addition to the ester gives an H-bonded adduct, $CH_{3-n}F_nCOOCH_3\cdots HOCH_3$, as a stable minimum, in which the alcohol H atom interacts with the acetate carbonyl O atom and the alcohol O atom is correctly placed on top of the ester carbonyl C atom to perform the nucleophilic addition. This minimum is stabilized relatively to the separated reagents on the electronic energy scale, but endoergic on the Gibbs energy scale. The TS and local minimum for the resulting tetrahedral intermediate $CH_{3-n}F_nC(OH)(OCH_3)_2$ were located for all *n* values. The height of the Gibbs energy barrier decreases as the F substitution (*n* value) increases, the highest

drop being observed between the CH_2F and the CHF_2 system, but the absolute values are unreasonably high (34-37 kcal mol^{-1} range, see Figure S1). This was expected, since the proton transfer occurs via a strained 4-member cycle with an unfavorable geometry for the H-bond stabilization. The calculations were therefore repeated for a system that includes a second alcohol molecule as a proton relay. As expected, the reaction barriers are dramatically reduced, see Figure 1.

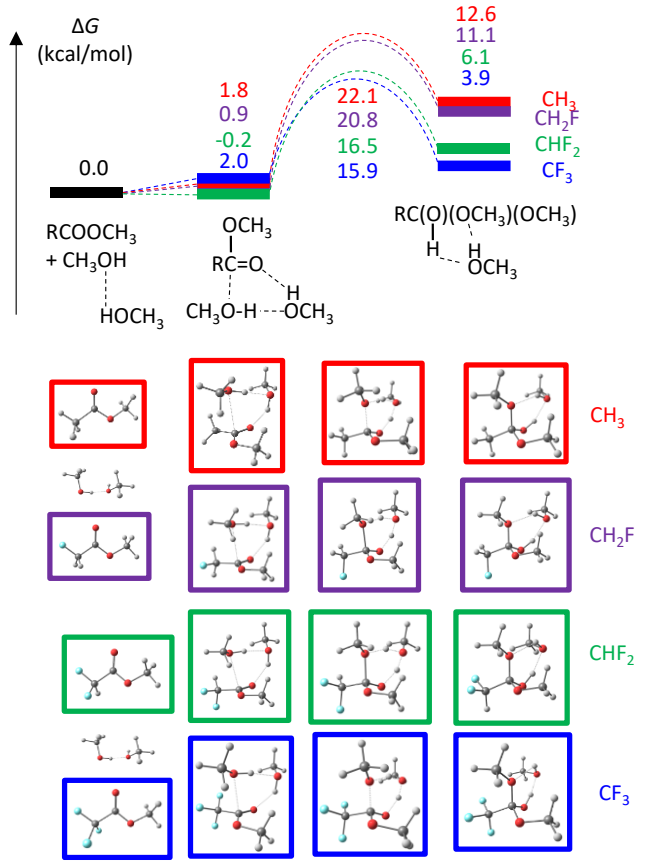

Figure 1. Gibbs energy profile (relative G298K,1M values in kcal mol^{-1}) for the MeOH addition to $CH_{3-n}F_nCOOCH_3$ (n = 0-3) with inclusion of an additional MeOH molecule as proton relay.

The starting point of the reaction is the combination of the separate ester and MeOH dimer, $(MeOH)_2$, in which there is an H-bond between the proton one MeOH molecule and the O atom of the second one. The two partners form an adduct, which is nearly isoergic with the separate partners, where the "free" $(MeOH)_2$ proton docks onto the ester carbonyl O atom and the O atom of the second MeOH molecule faces the ester carbonyl C atom, ready for the nucleophilic addition. The transition state energy is located at an energy in the 15.9-22.1 kcal mol^{-1} range relative to the separate fragments and becomes smaller as the F substitution on the ester increases. The tetrahedral intermediate is located at a relative energy in the 3.9-12.6 kcal mol^{-1} range and is also more stabilized for greater F substitutions. Like for the trend outlined above in the absence of the second alcohol molecule, the barrier drop is most significant on going from the CH_2F to the CHF_2 system, whereas the barrier reductions for the CH_3/CHF_2 and CHF_2/CF_3 pairs are smaller.

In terms of the transesterification process in the fluorinated vitrimers, these calculations suggest not only that the F inclusion at the ester α position is beneficial, particularly on going from CHF to CF_2, but also that the process should become more favorable when a larger excess of free alcohol functions are available in proximity of the reacting ester and alcohol groups. Given the established H-bond chain effect, all subsequent calculations were only carried out with inclusions of two alcohol molecules.

Effects of α-F and β-F substitution in propionate esters.

Additional calculations aimed at probing the generality of the α-F substitution effect and to explore in greater details the already established[18] β-F substitution effect on the transesterification barrier. The overall numerical results are summarized in Table 1. Views of the reaction profiles and of the optimized geometries are available in the Supporting Information (Figure S2, Figure S3 and Figure S4 for the CH_2, CHF and CF_2 systems, respectively).

Table 1. Gibbs energies ($\Delta G_{298K,1M}$ in kcal mol^{-1}), relative to the separate reagents for the methanol addition from $(CH_3OH)_2$ to $CH_{3-n}F_nCH_{2-m}F_mCOOCH_3$.Table Caption.

n	*m*	Adduct	TS	Tetrahedral Intermediate
0	0	0.1	23.0	15.6
1		0.3	21.9	14.5
2		-0.7	19.9	11.7
3		-0.9	21.7	12.8
0	1	1.2	21.2	12.9
1		1.0	19.4	12.1
2		0.5	19.9	11.7
3		0.8	20.1	11.2
0	2	0.1	16.8	8.0
1		-0.6	17.0	7.9
2		-0.8	15.2	6.4
3		-0.2	16.2	8.1

The analysis of the activation barriers (TS energy relative to the starting reagents), which can better be visualized in the graphical representation of Figure 2, shows that the effect of the α-C substitution (m) is qualitatively identical to that in the acetate esters analysed in the previous section, with a slight drop for the CH_2/CHF pair and a bigger on for the CHF/CF_2 pair. The F substitution at the β-C atom, on the other hand, has a much smaller and non-monotonous effect. There is a slight decrease of the activation barrier on going from CH_3 to CF_3 in this position, but the lowest barrier is associated to either CF_3 or CHF_2, depending on the F substitution at the α-C atom.

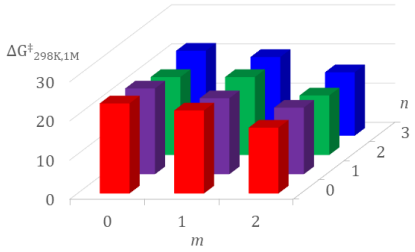

Figure 2. Transition state Gibbs energy (in kcal mol^{-1}) as a function of *n* and *m* for the transesterification of $CH_{3-n}F_nCH_{2-m}F_mCOOCH_3$ (*n* = 0-3, *m* = 0-2) with inclusion of an additional MeOH molecule as proton relay.

The structural analysis of the transition state as a function of *n* and *m* (Figure 3; data are in the Supporting Information, Table S1) reveals a few interesting trends. The Mulliken charge on the carbonyl C atom, contrary to expectations, does not increase with the F substitution. Conversely, the cumulative charge for the $(MeOH)_2$ fragment increases, particularly as a function of *m* (0.38-0.47 for α-CH_2, 0.44-0.49 for α-CHF, 0.50-0.53 for α-CF_2, the exact value depending on the number of β-F substituents, *n*). This trend is paralleled by a significant decrease and increase for the O···H distances E and F, respectively, and by a decrease of the C···O distance B, whereas the O···H distances C and D are much less affected. These trends indicate an increased ionic character, $[R_FC(OMe)_2O^-\cdots(MeOH_2)^+]$, for the transition state, namely an earlier methoxide transfer to the ester carbonyl C atom than the proton transfer to the carbonyl O atom. This is also consistent with the reduced degree of the C=O bond (A) lengthening from the free ester values (1.215-1.244 Å, shorter for more F-substituted esters). This phenomenon rationalizes the relative invariance of the carbonyl C atom electron density at the TS level and confirms the enhanced ester carbonyl electrophilicity as a result of the F substitution. The increase of the F substitution and corresponding TS stabilization results, in addition, in the shallowing of the potential energy surface at the TS level, namely a lower imaginary frequency (curvature along the reaction coordinate at the saddle point), by a factor of almost 2 between the two extremes (1117.8i cm^{-1} for $CH_3CH_2COOCH_3$ *vs.* 679.3i cm^{-1} for $CF_3CF_2COOCH_3$).

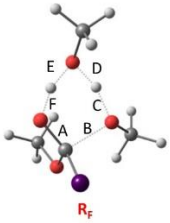

Figure 3. Structural parameters for the geometric analysis of the transition state of the degenerate transesterification of propionate esters by methanol, with inclusion of an additional MeOH molecule as proton relay (R_F = $CH_{3-n}F_nCH_{2-m}F_m$; *n* = 0-3, *m* = 0-2).

Effects of the F substitution on the alcohol reagent.

It was also of interest to probe whether the transesterification would be accelerated if the F substituents are placed on the alcohol part. For this purpose, the degenerative exchange was also probed for the acetate esters of differently F-substituted methanols, $CH_{3-n}F_nOH$ (n = 0-3). From the results of this investigation (details in Figure S5), it appears that this F substitution does not enhance the exchange rate. Strangely, the introduction of the first F atom (CH_2FOH) stabilizes both the H-bonded adduct and the tetrahedral intermediate. Consequently, the TS energy (relative to the separated reagents, CH_3COOCH_2F + $CH_2FOH\cdots O(H)CH_2F$) is also lower. However, the barrier from the H-bonded adduct is greater than that of the non-substituted ester. The barrier then further increases for the CHF_2OH and CF_3OH degenerative exchange processes (only slightly for CF_3OH and much more for CHF_2OH). The TS geometry analysis (Figure 4; data in the Supporting Information, Table S2) again shines light on the dynamics of this transesterification process. In this case, the $[ROH_2]$ unit is not increasing its charge upon increasing the F substitution. Rather, it decreases it. It seems, on the other hand, that the introduction of F groups on the alcohol induces an increased tendency to transfer a proton to the carbonyl function, to formally obtain a $[CH_3C(OH)(OR)]^+[RO\cdots H\cdots OR]^-$ structure, before transferring the alkoxide to the carbonyl C atom. This is clearly shown by the decrease of the F and D distances, by the increase of the B and E distances, and by the increase of the negative charge of the (ROHOR) fragment at the transition state level. In addition, the imaginary frequency drops from the CH_3 (1127.8i cm^{-1}) and CH_2F (1136.6i cm^{-1}) systems on one side, to the CHF_2 (124.7i cm^{-1}) and CF_3 (162.3i cm^{-1}) systems on the other one. In fact, the imaginary vibrational mode for the first two systems has the greatest component from the D shortening and E lengthening, whereas the last two systems show a much greater contribution from the B shortening and the C lengthening. Attemps to locate a possible charge-separated intermediate with the homoconjougate $(ROHOR)^-$ anion were not successful.

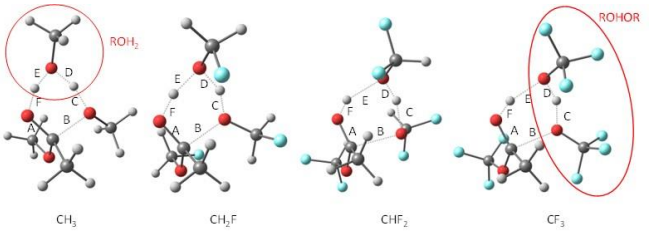

Figure 4. Structural parameters for the geometric analysis of the transition state of the degenerate transesterification of acetate esters of fluorinated alcohols R_FOH (R_F = $CH_{3-n}F_n$; *n* = 0-3), with inclusion of an additional R_FOH molecule as proton relay.

Experimental kinetic studies

The above-described DFT calculation results suggest that the strongest accelerating effect in transesterification should occur for a double H/F substitution at the ester α-C atom, whereas substitution at the β-C atom, though still providing an accelerating effect, is predicted to be less important and substitution in the alcohol part conversely induces a retardation effect. In order to check the reliability of these predictions, kinetic measurements of reaction rates and activation barriers have been conducted on a few model compounds, using conditions (solvent permittivity) as close as possible to those used in the vitrimer network and in the computational study.

A small set of easily accessible ethyl or methyl α,α-difluorinated esters was selected, as well as their hydrogenated counterparts, to first explore the feasibility of the trans-esterification reaction with a heavier primary alcohol, *n*-hexanol (Figure 5). A large excess (at least 10 equivalents) of this

competing alcohol was used, at the same time keeping the alcohol concentration approximately constant and shifting the equilibrium in favour of the heavier ester product, hence removing the need to include reversibility in the kinetic analysis, at least up to relatively high conversions.

Preliminary study

Propionates **1**-H and **1**-F were first tested in preliminary experiments using 10 equivalents of *n*-hexanol and CH_2Cl_2 as solvent, resulting in no conversion at room temperature. Therefore, the temperature was gradually raised under solvent-free conditions. A low conversion (8 %) could only be observed for the fluorinated ester **1**-F after 24 h at 100°C. These transesterification reactions were obviously slower than expected, requiring much higher temperatures than allowed by the substrate volatility for a proper kinetic investigation. Consequently, the less volatile ethyl 2,2-difluoro-2-phenylacetate **2**-F and the non-fluorinated methyl 2-phenylacetate **4**-H analogue were selected for further investigations without solvent and the reaction temperature was increased to 130 °C. Under these conditions, the transesterification of **2**-F with *n*-hexanol reached a 78.6 % conversion after 24 h and a GC/MS monitoring of the product concentrations in the presence of an internal standard (see data in Table S4) allowed us to depict a first kinetic profile. The ln([**2**-F]/[**2**-F]$_0$) *vs.* time (pseudo-first order) plot gave a linear fit (Figure 6), yielding k_{obs} = (1.78±0.02)·10^{-5} s^{-1}. Given that the rate law is also first order in alcohol (as independently verified, see next section), the second-order rate constant $k_{2\text{-}F}$ for this substrate is calculated as (2.41±0.03)·10^{-6} L mol^{-1} s^{-1}. Under the same conditions, the transesterification of the non-fluorinated substrate **4**-H is much slower since only a 12% conversion was reached after 48 h and barely 47% after over 8 days. As for **2**-F, the reaction was monitored by GC/MS (data in Table S5), yielding again a linear first-order plot (Figure 6) with k_{obs} = (8.8±0.3)·10^{-7} s^{-1} and $k_{2\text{-}H}$ = (1.19±0.04)·10^{-7} L mol^{-1} s^{-1}. From these preliminary investigations, a strong positive kinetic effect of the fluorine substitution on the transesterification reaction ($k_{2\text{-}F}$ /$k_{2\text{-}H}$ = 20) was demonstrated. All rate constants determined in the present investigation are collected in Table 2.

Determination of the partial order in alcohol

The kinetic investigation was continued with the verification of the reaction order in alcohol for the transesterification of **2**-F. In order to vary [HexOH]$_0$ without changing [ester]$_0$, 1,2-dichlorobenzene (1,2-DCB; boiling point = 179 °C) was used as a solvent. This choice was based, besides its high boiling point, on the close value of its dielectric constant (ε = 9.93) to that use in the model DFT study. Using the same [HexOH]$_0$/[**2**-F]$_0$ ratio as in the solvent-free experiment, the kinetic profile is very similar, yielding k_{obs} = (5.40±0.05)·10^{-6} s^{-1} (data in Table S6). The same experiment was then conducted using [HexOH]$_0$/[**2**-F]$_0$ ratios of 15 and 20, yielding again excellent fits to the pseudo-first-order rate law with faster conversions, k_{obs} = (7.04±0.15)·10^{-6} and (1.02±0.01)·10^{-5}, respectively, see Figure 7. A plot of k_{obs} *vs.* [HexOH] yields a linear correlation as expected for a first-order dependence (Figure 8), yielding $k_{2\text{-}F}$ = (2.02±0.13)·10^{-6} L mol^{-1} s^{-1}. The latter value is very close to that obtained in the solvent-free experiment, presumably because the dielectric constants of 1,2-dichlorobenzene is similar to that of *n*-hexanol (ε = 13.03).

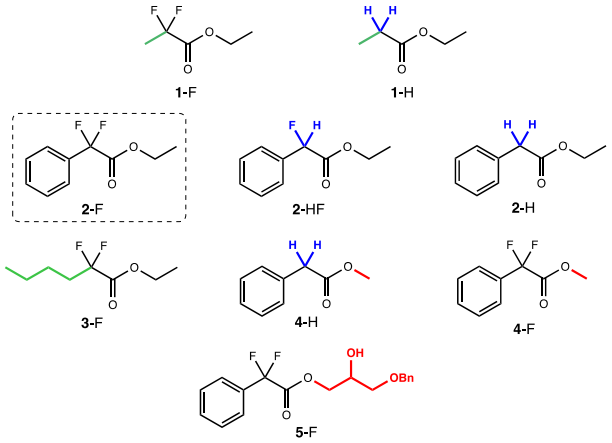

Figure 5. Esters used in the kinetic study.

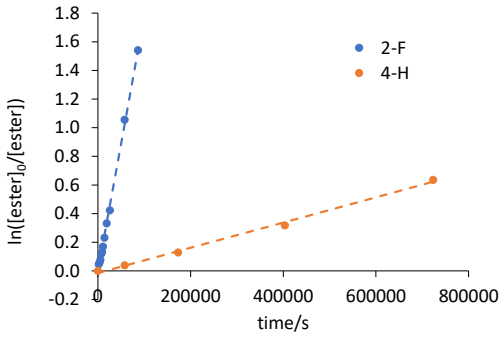

Figure 6. Pseudo-first order plot for the transesterification of **2**-F and **4**-H with *n*-hexanol at 130 °C. The dashed lines are the least-squares fits.

Table 2. Rate constants for the transesterification of various esters by excess *n*-hexanol.

Ester	Solvent	*T*/°C	k_{obs}/s^{-1}	[HexOH]$_0$	*k*/L mol^{-1} s^{-1}
2-F	-	130	(1.78±0.02)·10^{-5}	7.39	(2.41±0.03)·10^{-6}
4-H	-	130	(8.8±0.3)·10^{-7}	7.14	(1.23±0.04)·10^{-7}
2-F	1,2-DCB	130	(5.40±0.05)·10^{-6}	2.47	
2-F	1,2-DCB	130	(7.04±0.15)·10^{-6}	3.70	(2.02±0.13)·10^{-6}
2-F	1,2-DCB	130	(1.02±0.01)·10^{-5}	4.94	
2-HF	1,2-DCB	130	(2.55±0.07)·10^{-7}	2.51	(1.02±0.03)·10^{-7}
2-H	1,2-DCB	130	(1.08±0.04)·10^{-7}	2.51	(4.31±0.14)·10^{-8}
3-F	1,2-DCB	130	(3.63±0.06)·10^{-6}	2.51	(1.45±0.03)·10^{-6}
4-H	1,2-DCB	130	(1.64±0.08)·10^{-7}	2.51	(6.52±0.31)·10^{-8}
4-F	1,2-DCB	130	(6.66±0.16)·10^{-6}	2.51	(2.66±0.06)·10^{-6}
5-F	1,2-DCB	130	(2.17±0.03)·10^{-5}	2.51	(8.66±0.13)·10^{-6}
2-F	1,2-DCB	110	(6.90±0.08)·10^{-7}	2.51	(2.75±0.03)·10^{-7}
2-F	1,2-DCB	120	(1.89±0.01)·10^{-6}	2.51	(7.55±0.05)·10^{-7}
2-F	1,2-DCB	140	(5.25±0.09)·10^{-6}	2.51	(3.99±0.08)·10^{-6}

Influence of the carboxylate nature

Having established that the reaction follows a first order rate law on both transesterification partners, a comparative study was carried out with different esters RCX_2CO_2Et with variation of the fluorine substitution at the C^{α} atom (**2**-H, **2**-HF, **2**-F) and of the lateral chain (R = Ph or *n*-Bu; **2**-F *vs.* **3**-F). The transesterification reaction of **3**-F under standard conditions ($[\mathbf{3}\text{-F}]_0$ = 0.25 M, $[HexOH]_0$ = 2.50 M, 1,2-DCB, 130 °C; data in Table S7 and Figure S11) exhibited a kinetic profile very similar to **2**-F. The rate constant for **3**-F, $k_{\mathbf{3}\text{-F}}$ = (1.45±0.03)·10^{-6} L mol^{-1} s^{-1}, is only slightly smaller than that of the phenyl derivative (see Table 2), showing very little influence of the R group on the transesterification kinetics. The comparison of the differently F-substituted **2** derivatives at the C^{α} position (Table S8 and Figure S12) shows that the monofluorination has little influence on the rate of the reaction ($k_{\mathbf{2}\text{-HF}}/k_{\mathbf{2}\text{-H}}$ = 2.4) compared to the effect of difluorination ($k_{\mathbf{2}\text{-F}}/k_{\mathbf{2}\text{-H}}$ = 47).

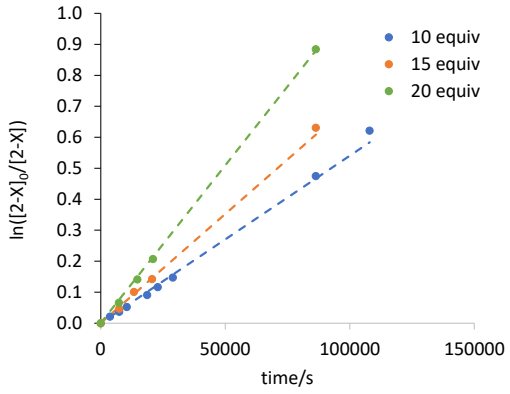

Figure 7. Pseudo-first order plots for the transesterification of **2**-F with *n*-hexanol at 130 °C with different $[HexOH]_0/[\mathbf{2}\text{-F}]_0$ ratios. The dashed lines are the least-squares fits.

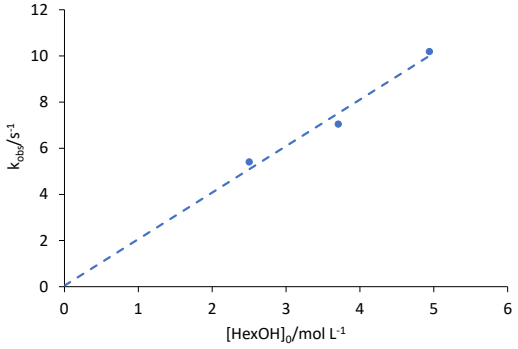

Figure 8. Dependence of k_{obs} (x10^6) on [HexOH] for the transesterification of **2**-F with *n*-hexanol at 130 °C. The dashed line is the least-squares fit.

Influence of the ester alkoxy moiety

The effect of the ester leaving group was also examined. We first checked that the length of a linear alkyl chain had little influence on the rate of the reaction. The methyl esters **4**-X (X = H, F; data in Table S9 and graphs in Figure S13) gave rate constants only slightly greater than those of the corresponding **2**-X ($k_{\mathbf{4}\text{-H}}/k_{\mathbf{2}\text{-H}}$ = 1.5; $k_{\mathbf{4}\text{-F}}/k_{\mathbf{2}\text{-F}}$ = 1.3), see Table 2, probably because of a slight steric effect of Et *vs.* Me.

The ester **5**-F was prepared by a catalyst-free epoxide ring-opening reaction between α,α-difluorophenylacetic acid and benzyl glycidyl ether (Scheme 2). This reaction is similar to that used for the preparation of our first fluorinated vitrimer, thus **5**-F features the same β-hydroxy group as in the vitrimer material.[17] The transesterification of **5**-F by *n*-hexanol (data in Table S10, pseudo-first order plot in Figure S14) revealed an interesting rate enhancement relative to the ethyl ester **2**-F, see Table 2 ($k_{\mathbf{5}\text{-F}}/k_{\mathbf{2}\text{-F}}$ = 4.3). This modest but sensible accelerating effect is most likely due to an electrophilic activation of the ester thanks to an intramolecular hydrogen bond between the carbonyl function and the β-hydroxy group, as also recently evidenced for the cyclic carbonate aminolysis.[23]

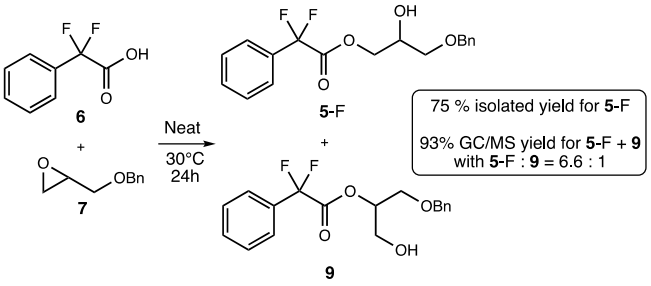

Scheme 2. Preparation of ester 5-F.

Influence of the competing alcohol

Finally, the influence of the steric hindrance of the alcohol nucleophile was also examined using 4-heptanol as the competing nucleophile for the transesterification of **2**-F (data in Table S11). As explained above, the vitrimer material was prepared by the opening of a monosubstituted epoxide (benzyl glycidyl ether) with an α,α-difluorinated acid (2,2-difluorophenylacetic acid), giving rise to the privileged, but not exclusive, formation of secondary alcohols such as in **5**-F. It was thus necessary to examine the reactivity of an alcohol modelling this kind of nucleophiles. The comparison of the transesterifications kinetics for ester **2**-F with 4-heptanol (k_{obs} = (1.31±0.03)·10^{-7} s^{-1}; $k_{\mathbf{2}\text{-F(4-HeptOH)}}$ = (5.35±0.14)·10^{-8} L mol^{-1} s^{-1}) and *n*-hexanol (Figure S19) clearly shows a severe drop in the reaction rate on going from the primary to the secondary alcohol ($k_{\mathbf{2}\text{-F(HexOH)}}/k_{\mathbf{2}\text{-F(4-HeptOH)}}$ = 38). Consequently, although the accelerating effect of the fluorine substitution on the transesterification reaction is clear, the result of this experiment raises questions on the nature of the exchange reactions occurring during the vitrimer material reshaping process. At least two hypotheses need consideration. First, it is plausible that the transesterification reaction involved in the early reprocessing of the material is due to the minority fraction of more reactive primary alcohols (such as in **9**) that are generated from the network synthesis (Scheme 3, path a). One should keep in mind that multiple transesterification reactions would result in the release of other primary alcohols and eventually in a possible statistical distribution of primary and secondary alcohols. Another possible reaction is the 1,2-migration of an ester group to the adjacent secondary alcohol, thus releasing a novel primary alcohol (Scheme 3, path b). However, we have never been able to observe such a migration at the molecular level and care must thus be taken to formulate this hypothesis for the material.

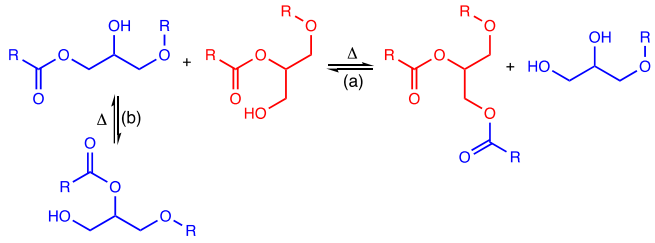

Scheme 3. Possible transesterification pathways in the material.

Determination of the activation enthalpy and entropy

The final part of the kinetic investigation dealt with the determination of the rate constant at different temperatures (110-140 °C range) for the transesterification of **2**-F, thus allowing the extraction of the activation parameters through the Eyring-Polanyi relationship for comparison with the computed values. In addition to the data at 130 °C already reported in Table S6, experiments were repeated at 110, 120 and 140 °C (data collected in Table S12 and pseudo-first order plots shown in Figure S20). The Eyring plot of the resulting second-order rate constants (Figure 9) shows a good linearity and the corresponding activation parameters can be extracted with confidence: $\Delta H^{\ddagger}$ = 27.7±1.4 kcal mol^{-1}; $\Delta S^{\ddagger}$ = -16.7±3.4 cal mol^{-1} K^{-1}. The negative activation entropy is as expected for a reaction with a strongly associative character at the transition state. The corresponding activation Gibbs energy, $\Delta G^{\ddagger}$, at 130 °C is 21.0 kcal mol^{-1}. The calculated values for the α-CF_2-containing model compounds CHF_2COOCH_3 and $CH_3CF_2COOCH_3$ under standard conditions (16.5 kcal mol^{-1} and 16.8 kcal mol^{-1}, respectively) after extrapolation to 130 °C, yield 22.3 kcal mol^{-1} for CHF_2COOCH_3 and 22.7 kcal mol^{-1} for $CH_3CF_2COOCH_3$, in relatively good agreement with the experimental value for the **2**-F/*n*-hexanol system.

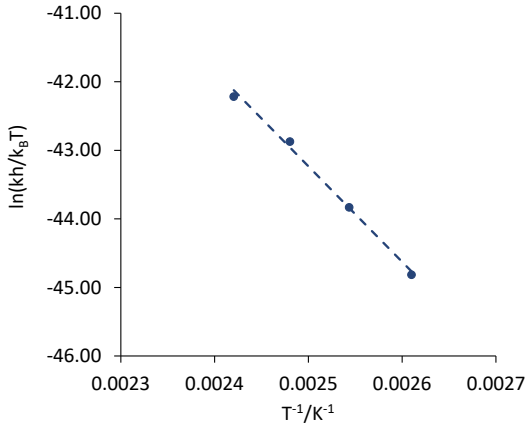

Figure 9. Eyring plot of the rate constants for the transesterification of **2**-F by *n*-hexanol in the 110-140 °C range. The dashed line is the least-squares fit and the red marks are the error bars based on the standard deviations.

Conclusion

The experimental investigation of the transesterification kinetics revealed a strong influence of α-difluorination on the reaction rate, whereas monofluorination exerts almost no effect (Scheme 4). These results qualitatively agree with predictions based on DFT calculations. We have confirmed that the nature of the R^1 group is not crucial (similar rate constants for **2**-F and **3**-F), thus the use of simple model ester substrates (R^1 = CH_3) should not introduce a strong bias in the DFT calculations. The kinetic study also highlighted an unexpected influence of a β-hydroxy group on the ester alkoxy chain, while the length of the same chain has a negligible effect. Finally, transesterification with a secondary alcohol proved to be much slower than with a primary alcohol. This combined DFT and experimental kinetic study of the transesterification reaction confirmed the primary hypothesis that initiated the preparation of fluorinated polyester vitrimers: a sufficient fluorination degree considerably enhances the transesterification reaction rate and this acceleration is most certainly responsible for the remarkable mechanical behaviour of our additive-free vitrimers. Not only was this confirmation necessary, the present study has also revealed other features and has raised a few questions regarding the discrepancies between the molecular reaction and the macromolecular behaviour.

First of all, we were surprised in our vitrimer study by the exceptional reactivity between our difluorinated triacid and the epoxy partner in a reaction which usually requires a catalyst and a high temperature.[17] The network was formed very quickly at room temperature without additive and this high reactivity was also observed at the molecular level between α,α-difluoro-α-phenylacetic acid and benzyl glycidyl ether. If the increased acidity of the carboxylic acid partner most probably accounts for this reactivity, a thorough study of this particular reaction is necessary to confirm this assumption.

Secondly, we were surprised in the early stage of our study by the differences between the exchange rate in our molecular models and the reshaping of our vitrimer material.[17] Vitrimers are characterized not only by their glass transition temperature (T_g, the temperature above which chain mobility in the material is possible) but also by their topology freezing transition temperature (T_v, the temperature above which exchange reactions are fast enough to decrease viscosity down to 10^{12} Pa.s).[1b] A vitrimer can be reprocessed above these two temperatures since both chain mobility and fast exchange reactions are required for that purpose. Our reported material has a low T_g (47°C) so transesterification reactions obviously occur (at least at a sufficient rate) far above this temperature, as illustrated by the temperature required for reshaping (100°C) and even more by the present experimental molecular study. Indeed, vigorous conditions and long reaction times are required here to perform a transesterification reaction, including with difluorinated esters. In contrast, our first material based on difluorinated esters could be rapidly reshaped at a temperature close to our reaction conditions at the molecular level.[17] Since molecular mobility above the T_g is obviously constrained in the material, this was a bit unexpected, though several hypotheses can explain the remarkable properties of the material.

Regarding the exchange reaction itself, the associative mechanism of the transesterification translates into a negative entropy of activation, confirmed experimentally by our kinetic study. A reasonable assumption would be that the volume of activation is also negative and that the reaction is accelerated at higher pressures, such as in the press used for the polymer reshaping. A supramolecular effect should also be taken into account, depending on the network density. Indeed, the material might also force the reactive functions to be closer to each other than what is possible in solution and therefore compensate the

lack of molecular mobility by a seclusion of the partners. However, these are only mere hypotheses, requiring more thorough studies for validation.

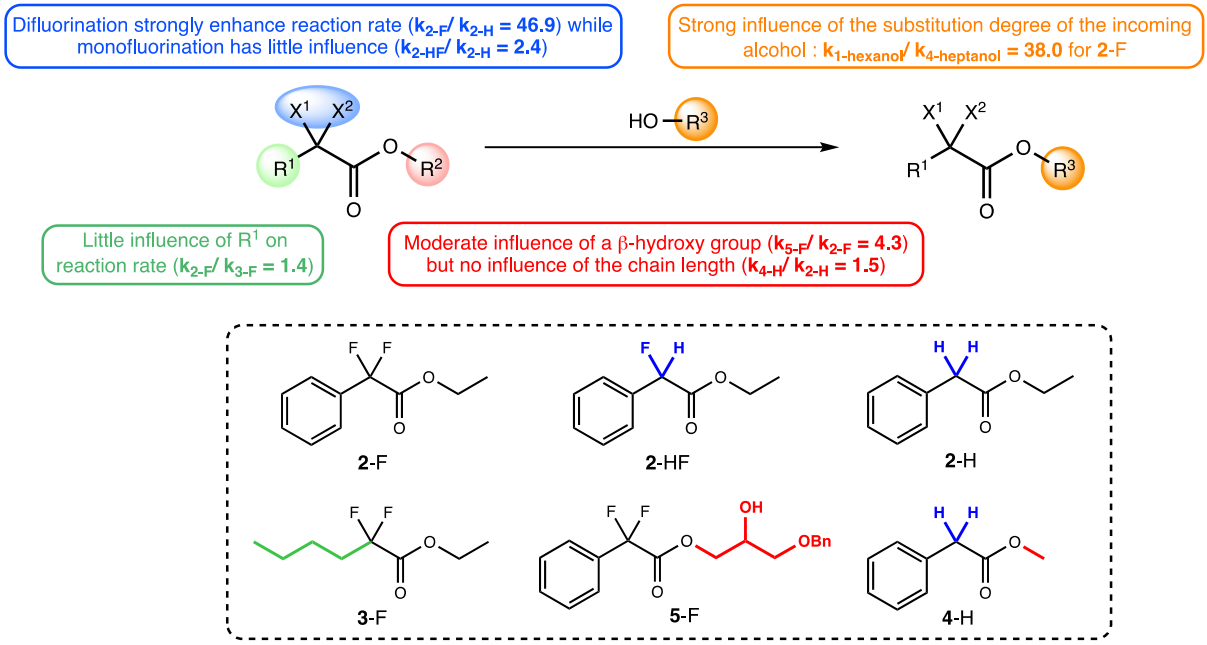

Scheme 4. Influence of the structural parameters on the transesterification rate.

Experimental Section

All the reactions were carried out in 10 mL microwave reaction vials with Teflon® cap and egg-shaped stirring bars purchased from VWR®. 1,3,5-trimethoxybenzene (99%), ethyl phenylacetate (99%), methyl phenylacetate (99%), anhydrous 1,2-dichlorobenzene (99%) and ReagentPlus® 1-hexanol (99.5%) were purchased from Sigma Aldrich® and used without further purification. Ethyl 2,2-difluorohexanoate (95%) was purchased from Fluorochem® and used without further purification. All the other starting esters were synthesized according to known procedures from the literature. ^{1}H and ^{13}C NMR spectra were recorded with a Bruker AC-400 MHz spectrometer in $CDCl_3$. For ^{1}H NMR (400 MHz), $CHCl_3$ and TMS served as internal standards (δ = 7.26 and 0 ppm) and data are reported as follows: chemical shift (in ppm), multiplicity (s = singlet, d = doublet, t = triplet, m = multiplet), coupling constant (in Hz), and integration. For ^{13}C NMR (100 MHz), $CHCl_3$ was used as internal standard (δ = 77.16) and spectra were obtained with complete proton decoupling. Gas chromatography–mass spectra (GC/MS) were recorded on a Shimadzu QP2012-SE with a Zebron ZB-5MS (20 m × 0,18 mm), capillary apolar column (Stationary phase: 0.18 µm film). GC/MS method: Initial temperature: 50 °C; Initial time: 2 min; Ramp: 22 °C/min; Final Temperature: 280 °C; Final time: 15 min. MS Spectra were recorded from 5.3 min to 15 min to avoid saturation of the spectrometer with 1-hexanol (3.5 min) and 1,2-dichlorobenzene (5.1 min).

Transesterification kinetics procedure: In a 10 mL microwave sealed vial were introduced the ester (0.25 mmol), the alcohol (2.5 mmol), the internal standard (1,3,5-trimethoxybenzene, 14.0 mg, 0.33 equiv) and a volume of 1,2-dichlorobenzene was added so that the total volume of the reaction mixture is 1.0 mL. The reaction was stirred at the given temperature (oil bath) and the conversion of the starting ester was monitored by GC/MS (aliquots of the reaction mixture were taken after cooling down the reaction to room temperature in a cold-water bath).

Computational details: The computational work was carried out using the Gaussian09 suite of programs.[24] The geometry optimizations were performed without any symmetry constraint using the BP86 functional and the 6-311G(d,p) basis functions for all atoms. The effects of dispersion forces (Grimme's D3 empirical method[25]) and solvation (SMD,[26] ε = 10) were included during the optimization. The ZPVE, PV, and TS corrections at 298 K were obtained with Gaussian09 from the solution of the nuclear equation using the standard ideal gas and harmonic approximations at T = 298.15 K, which also verified the nature of all optimized geometries as local minima or first-order saddle points. A correction of 1.95 kcal/mol was applied to all G values to change the standard state from the gas phase (1 atm) to solution (1 M).[27]

Acknowledgements

We thank the Agence Nationale de la Recherche (ANR) for fundings (AFCAN program, ANR-19-CE06-0014-02). FC thanks the Institut Carnot Chimie Balard Cirimat for funding (CatFreeCAN program). RP is grateful to the CALMIP mesocenter of the University of Toulouse for the allocation of computational resources. The authors also wish to thank Lise Reymond for assistance in performing the kinetic study of the transesterification of **4-H** in dichlorobenzene at 130 °C.

Keywords: covalent adaptable networks • DFT calculations • fluorine effect • transesterification kinetics • vitrimers

[1] a) C. J. Kloxin and C. N. Bowman, *Chem. Soc. Rev.* **2013**, *42*, 7161-7173; b) W. Denissen, J. M. Winne and F. E. Du Prez, *Chem. Sci.* **2016**, *7*, 30-38; c) J. M. Winne, L. Leibler and F. E. Du Prez, *Polym. Chem.* **2019**, *10*, 6091-6108.

[2] G. M. Scheutz, J. J. Lessard, M. B. Sims and B. S. Sumerlin, *J. Am. Chem. Soc.* **2019**, *141*, 16181-16196.
[3] C. J. Kloxin, T. F. Scott, B. J. Adzima and C. N. Bowman, *Macromolecules* **2010**, *43*, 2643-2653.
[4] C. Bowman, F. Du Prez and J. Kalow, *Polym. Chem.* **2020**, *11*, 5295-5296.
[5] a) Y. Chujo, K. Sada and T. Saegusa, *Macromolecules* **1990**, *23*, 2636-2641; b) X. X. Chen, M. A. Dam, K. Ono, A. Mal, H. B. Shen, S. R. Nutt, K. Sheran and F. Wudl, *Science* **2002**, *295*, 1698-1702; c) K. K. Oehlenschlaeger, J. O. Mueller, J. Brandt, S. Hilf, A. Lederer, M. Wilhelm, R. Graf, M. L. Coote, F. G. Schmidt and C. Barner-Kowollik, *Advanced Materials* **2014**, *26*, 3561-3566.
[6] D. Montarnal, M. Capelot, F. Tournilhac and L. Leibler, *Science* **2011**, *334*, 965-968.
[7] T. Liu, B. M. Zhao and J. W. Zhang, *Polymer* **2020**, *194*, 122392.
[8] a) N. J. Van Zee and R. Nicolay, *Progr. Polym. Sci.* **2020**, *104*; b) W. Alabiso and S. Schlogl, *Polymers* **2020**, *12*.
[9] X. X. Yang, L. Z. Guo, X. Xu, S. B. Shang and H. Liu, *Materials & Design* **2020**, *186*.
[10] W. Denissen, G. Rivero, R. Nicolay, L. Leibler, J. M. Winne and F. E. Du Prez, *Adv. Funct. Mater.* **2015**, *25*, 2451-2457.
[11] a) B. Hendriks, J. Waelkens, J. M. Winne and F. E. Du Prez, *ACS Macro Lett.* **2017**, *6*, 930-934; b) C. F. He, S. W. Shi, D. Wang, B. A. Helms and T. P. Russell, *J. Am. Chem. Soc.* **2019**, *141*, 13753-13757; c) J. Y. Wang, S. B. Chen, T. F. Lin, J. H. Ke, T. X. Chen, X. Wu and C. Lin, *RSC Adv.* **2020**, *10*, 39271-39276; d) J. J. Lessard, L. F. Garcia, C. P. Easterling, M. B. Sims, K. C. Bentz, S. Arencibia, D. A. Savin and B. S. Sumerlin, *Macromolecules* **2019**, *52*, 2105-2111.
[12] M. Guerre, C. Taplan, J. M. Winne and F. E. Du Prez, *Chem. Sci.* **2020**, *11*, 4855-4870.
[13] F. Van Lijsebetten, J. O. Holloway, J. M. Winne and F. E. Du Prez, *Chem. Soc. Rev.* **2020**, *49*, 8425-8438.
[14] F. Cuminet, S. Caillol, E. Dantras, E. Leclerc and V. Ladmiral, *Macromolecules* **2021**, *54*, 3927-3961.
[15] a) Q. A. Poutrel, J. J. Blaker, C. Soutis, F. Tournilhac and M. Gresil, *Polym. Chem.* **2020**, *11*, 5327-5338; b) F. I. Altuna, U. Casado, I. E. Dell'Erba, L. Luna, C. E. Hoppe and R. J. J. Williams, *Polym. Chem.* **2020**, *11*, 1337-1347; c) F. I. Altuna, C. E. Hoppe and R. J. J. Williams, *RSC Adv.* **2016**, *6*, 88647-88655; d) M. Hayashi, R. Yano and A. Takasu, *Polym. Chem.* **2019**, *10*, 2047-2056.
[16] a) D. O'Hagan, *Chem. Soc. Rev.* **2008**, *37*, 308-319; b) J.-P. Bégué and D. Bonnet-Delpon, *Bioorganic and Medicinal Chemistry of Fluorine*, John Wiley & Sons Inc., Hoboken, **2008**, p.
[17] F. Cuminet, D. Berne, S. Caillol, E. Dantras, C. Joly-Duhamel, E. Leclerc, S. Lemouzy and V. Ladmiral, **submitted**.
[18] D. Berne, F. Cuminet, S. Lemouzy, C. Joly-Duhamel, R. Poli, S. Caillol, E. Leclerc and V. Ladmiral, *Macromolecules* **2022**, *55*, 1669−1679.
[19] a) H. W. Horn, G. O. Jones, D. D. S. Wei, K. Fukushima, J. M. Lecuyer, D. J. Coady, J. L. Hedrick and J. E. Rice, *J. Phys. Chem. A* **2012**, *116*, 12389-12398; b) K. X. Li, Z. H. Yang, J. Zhao, J. X. Lei, X. L. Jia, S. H. Mushrif and Y. H. Yang, *Green Chem.* **2015**, *17*, 4271-4280; c) K. X. Li, Y. B. Yan, J. Zhao, J. X. Lei, X. L. Jia, S. H. Mushrif and Y. H. Yang, *Phys. Chem. Chem. Phys.* **2016**, *18*, 32723-32734; d) J. Q. Ng, H. Arima, T. Mochizuki, K. Toh, K. Matsui, M. Ratanasak, J. Y. Hasegawa, M. Hatano and K. Ishihara, *ACS Catal.* **2021**, *11*, 199-207; e) S. Bhusal, C. Oh, Y. J. Kang, V. Varshney, Y. X. Ren, D. Nepal, A. Roy and G. Kedziora, *J. Phys. Chem. B* **2021**, *125*, 2411-2424.
[20] M. V. Zabalov and R. P. Tiger, *Theoretical Chemistry Accounts* **2017**, *136*, 95/91-20.
[21] R. C. Weast, *CRC Handbook of Chemistry and Physics*, CRC Press, Cleveland, Ohio, **2015**, p.
[22] in *Honeywell Dielectric Constant Table*, *Vol.* https://www.honeywellprocess.com/library/marketing/tech-specs/Dielectric%20Constant%20Table.pdf.
[23] B. Quienne, R. Poli, J. Pinaud and S. Caillol, *Green Chem.* **2021**, *23*, 1678-1690.
[24] M. J. Frisch, G. W. Trucks, H. B. Schlegel, G. E. Scuseria, M. A. Robb, J. R. Cheeseman, G. Scalmani, V. Barone, B. Mennucci, G. A. Petersson, H. Nakatsuji, M. Caricato, X. Li, H. P. Hratchian, A. F. Izmaylov, J. Bloino, G. Zheng, J. L. Sonnenberg, M. Hada, M. Ehara, K. Toyota, R. Fukuda, J. Hasegawa, M. Ishida, T. Nakajima, Y. Honda, O. Kitao, H. Nakai, T. Vreven, J. A. Montgomery Jr., J. E. Peralta, F. Ogliaro, M. Bearpark, J. J. Heyd, E. Brothers, K. N. Kudin, V. N. Staroverov, R. Kobayashi, J. Normand, K. Raghavachari, A. Rendell, J. C. Burant, S. S. Iyengar, J. Tomasi, M. Cossi, N. Rega, N. J. Millam, M. Klene, J. E. Knox, J. B. Cross, V. Bakken, C. Adamo, J. Jaramillo, R. Gomperts, R. E. Stratmann, O. Yazyev, A. J. Austin, R. Cammi, C. Pomelli, J. W. Ochterski, R. L. Martin, K. Morokuma, V. G. Zakrzewski, G. A. Voth, P. Salvador, J. J. Dannenberg, S. Dapprich, A. D. Daniels, Ö. Farkas, J. B. Foresman, J. V. Ortiz, J. Cioslowski and D. J. Fox, *Gaussian 09, Revision D.01*, Gaussian, Inc., Wallingford CT, **2009**, p.
[25] S. Grimme, J. Antony, S. Ehrlich and H. Krieg, *J. Chem. Phys.* **2010**, *132*, 154104.
[26] A. V. Marenich, C. J. Cramer and D. G. Truhlar, *J. Phys. Chem. B* **2009**, *113*, 6378-6396.
[27] V. S. Bryantsev, M. S. Diallo and W. A. Goddard, III, *J. Phys. Chem. B* **2008**, *112*, 9709-9719.

Entry for the Table of Contents

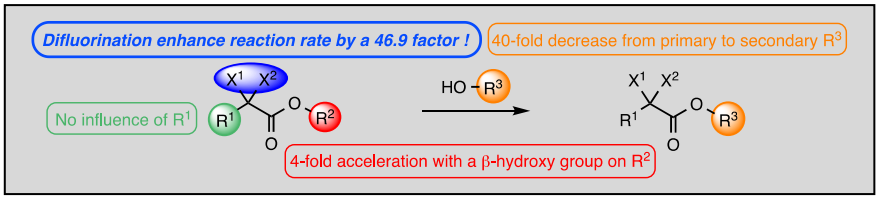

DFT calculations and an experimental kinetic study of a transesterification reaction were conducted in order to quantitatively assess the effect of neighbouring fluorinated groups on the reaction rate and provide a molecular model for the observed accelerating effect of proximal fluorinated groups in the reshaping of transesterification vitrimers.